Electronic states in impurity superlattices

Ahmet Elçi
Phillips Laboratory–LIDA, Kirtland Air Force Base, Albuquerque, New Mexico 87117
(Received 16 December 1991; revised manuscript received 30 March 1992)

This paper presents a band theory of impurity superlattices that takes into account the atomicity of impurity charges by using a Hamiltonian which is a functional of the probability distribution of donor and acceptor impurities. In this theory, subbands are generated from the symmetry breaking caused by the presence of impurities. Subband structure is determined by means of a canonical transformation. The analysis of electron-photon coupling shows that there is a hierarchy of selection rules for the $\mathbf{p}\cdot\mathbf{A}$ coupling of subbands.

I. INTRODUCTION

Impurity superlattices, referred to by some as doping superlattices and by others as *n-i-p-i* crystals, have been of great interest in recent years. A number of experiments have been reported concerning their optical and electronic properties. With some minor alterations, the basic theory used in the explanation of these properties has been that of Ruden and Döhler.[1–3] This theory is based upon the effective-mass approximation and the spatial continuity of charges whose potential field does not produce any interband coupling. The growing significance of impurity superlattices warrants a more rigorous analysis of their band structure and the verification or disproof of various physical pictures currently postulated in the literature. In this paper, I present a theory that takes into account the atomicity of impurity charges. This theory uses a canonical transformation to systematically disentangle the effects of a periodic impurity distribution on electronic states. It shows that the fundamental effect of impurities is to break the symmetry of the original crystal. Subbands are formed as a result of this symmetry breaking. The specific atomic properties of impurities play only a small role in the superlattice band structure. This result is consistent with observations to date that optical and electronic properties of impurity superlattices are determined by geometry, not by specific atomic properties. The mechanism of symmetry breaking requires reinterpretation of some of the experimental observations and makes predictions of other effects.

Section II discusses the Hamiltonian used in the analysis. This Hamiltonian describes the Coulomb interaction between electrons and impurities, as well as the coupling between electrons and light. It directly incorporates the probability distribution of impurities. I make a basic postulate that various crystal samples are identical, as far as the Hamiltonian is concerned, if they have the same probability distribution. I consider two types of probability distributions: a wavelike ($\cos^2$ and $\sin^2$) distribution of *n*- and *p*-type impurities within a superlattice cell (Fig. 1), and a piecewise-constant distribution (Fig. 2). The latter corresponds to the usual geometry discussed in theoretical papers. The former simplifies the algebra and the demonstration of subband formation. This interest in a wavelike probability distribution is not entirely pedagogical. Such superlattices may have interesting nonlinear properties for frequency up and down conversion of light.

In this paper I do not discuss the sawtooth superlattices which have δ-function distributions within a superlattice cell. The reason is that for the wavelike and piecewise-constant distributions, the analysis is best carried out in momentum space, using the momentum Bloch functions. For the sawtooth superlattices, the analysis should be carried out in ordinary space.

In the coupling of electrons to impurities, I assume that charges are screened and that the potential is Yukawa-type with an inverse screening length q_s. The screening wave vector q_s is extremely important, since it sets up the energy scale for various subband shifts. Although it is desirable to determine q_s self-consistently, using the subband structure in the Coulomb scattering of electrons, I do not attempt this laborious task in the present paper, but assume that q_s is a predetermined parameter for a given sample.

Section III discusses the formation of subbands for the wavelike distribution. As a result of the reduced symmetry, the original Brillouin zone (BZ) is partitioned into

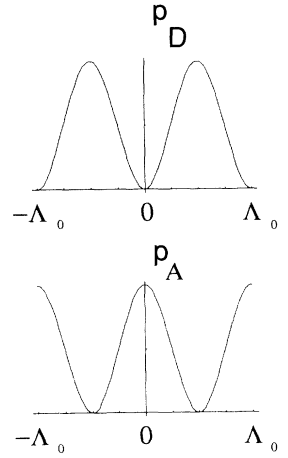

FIG. 1. A wavelike distribution for acceptors (p_A) and donors (p_D).

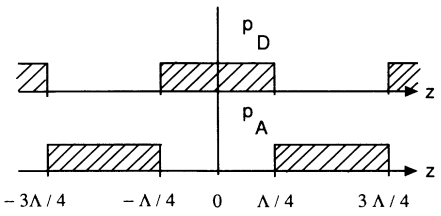

FIG. 2. A piecewise-constant-impurity distribution.

$2L-1$ pieces, where L is an integer given by the ratio of the modulation wavelength to the lattice constant of the pure crystal. There are L subbands of an original band in the superlattice BZ. A subband energy dispersion is determined essentially by the folding of the original BZ and the translation of the original energy bands to the superlattice BZ. When the electron-impurity coupling is rewritten in terms of the superlattice quantum numbers, one finds that the bands, as well as their subbands, are coupled. I remove this coupling systematically by means of a canonical transformation and determine the eigenenergies of the superlattice Hamiltonian to the second order in the impurity density. Although it may be redundant, I would like to point out that the discussion of this section is for those crystals in which an electron has an indefinitely large mean free path. When the electronic mean free path is finite, as for actual samples, the formation of the subband structure depends on the ratio of the mean free path to the superlattice modulation wavelength. If this ratio is much larger than 1, subbands will be observable in the single-particle spectrum of that sample. If the ratio is less than 1, subbands will not be observable.

Section IV discusses the electron-photon-coupling Hamiltonians for the wavelike distribution. In the approximation in which radiative recoils are neglected, the linear electron-photon-coupling Hamiltonian exhibits a hierarchy of selection rules. This differs from the quantum tunneling picture of electron-hole recombination or creation, in which there is no selection rule.[4] In contrast to the linear-coupling Hamiltonian, the quadratic electron-photon-coupling Hamiltonian, which determines light scattering from a plasma, remains unchanged to the order to which the canonical transformation is carried out.

Section V discusses the piecewise-constant-impurity distribution. Its results differ from Ref. 1 in that in the present theory, the energy scale for subband separations is set by the folding of the BZ, and the scale for subband shifts associated with the Coulomb scattering is set by the screening length. In the coupling to light, one again encounters a hierarchy of selection rules. Some concluding remarks are given in Sec. VI.

II. HAMILTONIAN

The Hamiltonian that includes the Coulomb interaction between electrons and impurities as well as the coupling to the electromagnetic field may be written as

$$H=H_e+H_i+H_\gamma+H_{e\gamma}+H_{e\gamma\gamma} . \tag{2.1}$$

H_e is the Bloch Hamiltonian with the periodic crystal potential $V(\mathbf{x})$:

$$H_e=\int d\mathbf{x}\,\psi^\dagger(\mathbf{x})\left[\frac{\mathbf{p}^2}{2m}+V(\mathbf{x})\right]\psi(\mathbf{x}) = \sum_b E_b^0 c_b^\dagger c_b . \tag{2.2}$$

b stands for the Bloch state $(n\mathbf{k}s)$, where n designates the bands, $\mathbf{k}$ the electronic momenta, and s the spins. m is the ordinary electron mass. E_b^0 is the Bloch energy. $\psi(\mathbf{x})$ is the electron-field operator:

$$\psi(\mathbf{x})=\sum_b \psi_b(\mathbf{x})c_b . \tag{2.3}$$

$\psi_b(\mathbf{x})$ are the Bloch functions. $c_b, c_b^\dagger$ are the anticommuting creation and annihilation operators. H_i describes the coupling between electrons and fixed impurities. For a given probability distribution of impurities, it is given by

$$H_i=\sum_j \int d\mathbf{r}\int d\mathbf{x}\,p_j(\mathbf{r})\psi^\dagger(\mathbf{x})v_j(\mathbf{x}-\mathbf{r})\psi(\mathbf{x}) = \sum_{b,b'} W_{bb'}c_b^\dagger c_{b'} . \tag{2.4}$$

The subscript j in (2.4) denotes the impurity type: $j=A,D$, where A stands for acceptors and D for donors. $p_j(\mathbf{r})$ is the probability that a j-type impurity will be found at $\mathbf{r}$. When p_j is integrated over the entire volume, one obtains the total number of the j-type impurities in the crystal:

$$\int d\mathbf{r}\,p_j(\mathbf{r})=V_{o1}N_j , \tag{2.5}$$

where N_j is the impurity density per unit volume. $v_j(\mathbf{x}-\mathbf{r})$ is the electrostatic potential of the impurity located at $\mathbf{r}$. I assume that it is a screened Coulomb potential

$$v_j(\mathbf{y})=e^2Z_j\frac{e^{-q_s y}}{\epsilon_0 y} . \tag{2.6}$$

Here e is the electronic charge, q_s is the screening wave vector, and ϵ_0 is the static dielectric constant. If the impurities are singly ionized, then Z_j is $+1$ for acceptors and -1 for donors. H_γ is the electromagnetic-field Hamiltonian

$$H_\gamma=\sum_\mu \hbar\omega_\mu a_\mu^\dagger a_\mu . \tag{2.7}$$

$a_\mu^\dagger, a_\mu$ are the photon creation and annihilation operators for the mode μ. $H_{e\gamma}$ is the electron-photon coupling arising from $\mathbf{p}\cdot\mathbf{A}$:

$$H_{e\gamma}=\sum_{b,b'\mu}[g_{bb'}^\mu c_b^\dagger c_{b'}a_\mu+\text{H.c.}] , \tag{2.8a}$$

$$g_{bb'}^\mu=\frac{e}{mc}A_\mu\langle b|e^{i\mathbf{q}_\mu\cdot\mathbf{x}}\boldsymbol{\epsilon}_\mu\cdot\mathbf{p}|b'\rangle , \tag{2.8b}$$

$$A_\mu=\left[\frac{2\pi\hbar c^2}{V_{o1}n_\mu^2\omega_\mu}\right]^{1/2} , \tag{2.8c}$$

where c is the speed of light, $\mathbf{p}$ is the momentum operator, $\boldsymbol{\varepsilon}_\mu$ is the unit polarization vector, $\mathbf{q}_\mu$ is the mode wave vector, n_μ is the index of refraction, and ω_μ is the mode frequency. If radiative recoil is neglected,

$$g^{\mu}_{bb'}=\frac{e}{mc}A_\mu\boldsymbol{\varepsilon}_\mu\cdot\mathbf{p}_{bb'}\ , \tag{2.9a}$$

$$\mathbf{p}_{bb'}=\langle b|\mathbf{p}|b'\rangle=\delta_{ss'}\delta_{kk'}\mathbf{p}_{nn'}(\mathbf{k})\ . \tag{2.9b}$$

$H_{e\gamma\gamma}$ describes the electron-photon coupling arising from $\mathbf{A}^2$:

$$H_{e\gamma\gamma}=\sum_{b,b'\mu\mu'}\{[d^{\mu\mu'}_{bb'}(\mathbf{q}_\mu+\mathbf{q}_{\mu'})a_\mu a_{\mu'} +d^{\mu\mu'}_{bb'}(\mathbf{q}_\mu-\mathbf{q}_{\mu'})a_\mu a^\dagger_{\mu'}]c^\dagger_b c_{b'}+\text{H.c.}\}\ , \tag{2.10a}$$

where

$$d^{\mu\mu'}_{bb'}(\mathbf{Q})=\frac{e^2}{2mc^2}\boldsymbol{\varepsilon}_\mu\cdot\boldsymbol{\varepsilon}_{\mu'}A_\mu A_{\mu'}\langle b|e^{i\mathbf{Q}\cdot\mathbf{x}}|b'\rangle\ . \tag{2.10b}$$

If radiative recoil is neglected, (2.10b) simplifies to

$$d^{\mu\mu'}_{bb'}(0)=\frac{e^2}{2mc^2}\boldsymbol{\varepsilon}_\mu\cdot\boldsymbol{\varepsilon}_{\mu'}A_\mu A_{\mu'}\delta_{bb'}\ . \tag{2.10c}$$

The coupling Hamiltonian H_i contains an average over the distribution of impurities. It therefore differs from a conventional impurity Hamiltonian. In the conventional method, one postulates a definite configuration for the impurities of a crystal sample and evaluates some Hermitian operator for this configuration. At the end of the calculation, one averages over various configurations to obtain quantities that are directly compared with experimental observations. Mathematically, the conventional method corresponds to

$$\bar{O}=\sum_c P_c O[C]\ , \tag{2.11}$$

where C denotes a definite configuration, P_c is its probability, and O is a Hermitian operator (or its quantum-mechanical expectation value). The conventional method is inspired by classical stochastic problems and $\bar{O}$, rather than O, is assumed to be the actual physical observable. $\bar{O}$ is compared with experiment even when observations are continuous and on the same sample, which precludes an ensemble average like (2.11). Note that the time evolution of $\bar{O}$ cannot be quantum mechanical, since

$$i\hbar\frac{\partial}{\partial t}\bar{O}=\sum_c P_c[H[C],O[C]]\ . \tag{2.12}$$

The right-hand side of (2.12) cannot be represented as the commutator of $\bar{O}$ with an effective Hamiltonian unless

$$\overline{OH}=\bar{O}\bar{H},\quad \overline{HO}=\bar{H}\bar{O}\ . \tag{2.13}$$

In general, this is not satisfied except for trivial operators. The difficulty with the meaning of $\bar{O}$ when it is used in conjunction with continuous observations has been known for many years. It is discussed, for example, by Kubo in his classic paper on irreversibility.[5]

In contrast, H_i of Eq. (2.4), hence H, is an "average" operator. The commutator of H with a Hermitian operator generates a proper quantum-mechanical time evolution while taking into account the randomness in impurity locations. There are several other reasons to prefer the present form for H. First, the Hamiltonian is the most fundamental observable of a physical object, determining the object's observable states. Self-consistency requires that if an average is to be performed on observable operators of a physical system or on their expectation values, the Hamiltonian must be first on the list. Second, the incorporation of impurity distributions into the Hamiltonian is analogous to the Kadanoff transformations of the renormalization group, which produce appropriate Hamiltonians near phase transitions. Third, the use of the present form for H avoids the difficulties of the quantum-mechanical interpretation. If various crystal samples have the same impurity distribution $\{p_j(\mathbf{r})\}$, then they are identical as far as the Hamiltonian is concerned. Thus $\{p_j(\mathbf{r})\}$ defines an identity class. One can determine whether a given sample belongs to this class by dividing it into several regions and comparing impurity locations in these regions. If a particular sample belongs to the class of $\{p_j(\mathbf{r})\}$, then its structure and evolution are determined by H. Experimental measurements determine the properties of the eigenstates of H. It does not matter whether experimental observations are made continuously on one sample or on many samples, as long as the samples belong to the same identity class.

Note that H_i reduces to the Hamiltonian of the conventional method if the impurity configuration is definite. If, with probability one, the acceptors are located at . . ., $\mathbf{r}_a,\mathbf{r}_{a+1},\ldots$ and the donors at . . ., $\mathbf{r}_d,\mathbf{r}_{d+1},\ldots$, then their distribution is given by

$$p_A(\mathbf{r})=\sum_a\delta(\mathbf{r}-\mathbf{r}_a)\ , \tag{2.14a}$$

$$p_D(\mathbf{r})=\sum_d\delta(\mathbf{r}-\mathbf{r}_d)\ , \tag{2.14b}$$

and H_i becomes

$$H_i=\int d\mathbf{x}\,\psi^\dagger(\mathbf{x})\left[\sum_a v_A(\mathbf{x}-\mathbf{r}_a) +\sum_d v_D(\mathbf{x}-\mathbf{r}_d)\right]\psi(\mathbf{x})\ , \tag{2.14c}$$

which is the conventional impurity-coupling Hamiltonian.

It is useful to express H_i of Eq. (2.4) in terms of momentum Bloch functions for later calculations. The momentum Bloch functions are related to the ordinary Bloch functions by

$$\psi_{n\mathbf{k}}(\mathbf{x})=\sum_G e^{i(\mathbf{k}-\mathbf{G})\cdot\mathbf{x}}\phi_n(\mathbf{k}-\mathbf{G})\ , \tag{2.15}$$

where $\mathbf{G}$ stands for reciprocal lattice vectors. ϕ_n are the momentum Bloch functions[6] with the orthogonality and completeness relations

$$\sum_G \phi_n^*(\mathbf{k}-\mathbf{G})\phi_{n'}(\mathbf{k}-\mathbf{G})=\delta_{nn'} , \tag{2.16a}$$

$$\sum_n \phi_n^*(\mathbf{k}-\mathbf{G})\phi_n(\mathbf{k}-\mathbf{G}')=\delta_{GG'} . \tag{2.16b}$$

Equations (2.15)–(2.16b) assume that the spin-orbit coupling of the crystal is weak and that the spin wave functions may be separated from the spatial Bloch functions. Then the spin index becomes degenerate and explicit references to spin may be omitted. Using (2.15) in (2.4), one finds

$$W_{n\mathbf{k};n'\mathbf{k}'}=\sum_{\mathbf{G},\mathbf{G}'}\phi_n^*(\mathbf{k}-\mathbf{G})\phi_{n'}(\mathbf{k}'-\mathbf{G}') \times\left[\sum_j P_j(\mathbf{k}-\mathbf{k}'-\mathbf{G}+\mathbf{G}') \times V_j(\mathbf{k}-\mathbf{k}'-\mathbf{G}+\mathbf{G}')\right] , \tag{2.17a}$$

where

$$V_j(\mathbf{Q})=\int d\mathbf{y}\, e^{-i\mathbf{Q}\cdot\mathbf{y}}v_j(\mathbf{y}) , \tag{2.17b}$$

$$P_j(\mathbf{Q})=\int d\mathbf{y}\, e^{-i\mathbf{Q}\cdot\mathbf{y}}p_j(\mathbf{y}) . \tag{2.17c}$$

For the screened Coulomb potential of (2.6), $W_{bb'}$ becomes

$$W_{n\mathbf{k};n'\mathbf{k}'}=\frac{4\pi e^2}{\epsilon_0}\sum_{\mathbf{G},\mathbf{G}'}\phi_n^*(\mathbf{k}-\mathbf{G})\phi_{n'}(\mathbf{k}'-\mathbf{G}') \times\left[\frac{\sum_j Z_j P_j(\mathbf{k}-\mathbf{k}'-\mathbf{G}+\mathbf{G}')}{[(\mathbf{k}-\mathbf{k}'-\mathbf{G}+\mathbf{G}')^2+q_s^2]}\right] . \tag{2.18}$$

Section III will be concerned with a wavelike impurity distribution. Let $Z_A=-Z_D=1$, $N_A=N_D=N_0$, and

$$p_A(\mathbf{r})=N_0[1+\cos(\mathbf{q}_0\cdot\mathbf{r})] , \tag{2.19a}$$

$$p_D(\mathbf{r})=N_0[1-\cos(\mathbf{q}_0\cdot\mathbf{r})] . \tag{2.19b}$$

Then $W_{bb'}$ becomes

$$W_{n\mathbf{k};n'\mathbf{k}'}=W_0\sum_{\mathbf{G},\mathbf{G}'}\phi_n^*(\mathbf{k}-\mathbf{G})\phi_{n'}(\mathbf{k}'-\mathbf{G}') \times[\delta_{\mathbf{k}-\mathbf{G}-\mathbf{k}'+\mathbf{G}',\mathbf{q}_0} +\delta_{\mathbf{k}-\mathbf{G}-\mathbf{k}'+\mathbf{G}',-\mathbf{q}_0}] , \tag{2.20a}$$

where

$$W_0=\frac{4\pi N_0 e^2}{\epsilon_0(q_0^2+q_s^2)} . \tag{2.20b}$$

Note that $\mathbf{k}$ and $\mathbf{k}'$, as well as $\mathbf{q}_0$, fall into the first Brillouin zone. The delta functions in (2.20a) may be satisfied only if $\mathbf{G}=\mathbf{G}'$:

$$\delta_{\mathbf{k}-\mathbf{G}-\mathbf{k}'+\mathbf{G}',\pm\mathbf{q}_0}=\delta_{\mathbf{G}\mathbf{G}'}\delta_{\mathbf{k}-\mathbf{k}',\pm\mathbf{q}_0} . \tag{2.21}$$

$W_{bb'}$ simplifies to

$$W_{n\mathbf{k};n'\mathbf{k}'}=W_0[\Phi_{nn'}(\mathbf{k}';\mathbf{q}_0)\delta_{\mathbf{k}-\mathbf{k}',\mathbf{q}_0} +\Phi^*_{n'n}(\mathbf{k};\mathbf{q}_0)\delta_{\mathbf{k}-\mathbf{k}',-\mathbf{q}_0}] , \tag{2.22a}$$

where

$$\Phi_{nn'}(\mathbf{k};\mathbf{q})=\sum_{\mathbf{G}}\phi_n^*(\mathbf{k}+\mathbf{q}-\mathbf{G})\phi_{n'}(\mathbf{k}-\mathbf{G}) . \tag{2.22b}$$

Note that W_0 corresponds to V_0 in the theory of Ruden and Döhler.[1] If one assumes that (2.19) represent a continuous charge distribution, then the Poisson equation

$$\nabla^2 V(\mathbf{r})=-\frac{8\pi N_0 e^2}{\epsilon_0}\cos(\mathbf{q}_0\cdot\mathbf{r}) \tag{2.23a}$$

yields

$$V(\mathbf{r})=\frac{8\pi N_0 e^2}{\epsilon_0 q_0^2}\cos(\mathbf{q}_0\cdot\mathbf{r})=2W_0'\cos(\mathbf{q}_0\cdot\mathbf{r}) , \tag{2.23b}$$

where W_0' is the amplitude of the potential modulation and corresponds to V_0 of Ref. 1. When the screening is included, q_0^2 is replaced by $q_0^2+q_s^2$ in (2.23b) and W_0' becomes W_0

III. FORMATION OF SUPERLATTICE SUBBANDS

In the manufacture of impurity superlattices, impurity concentration is regulated in individual atomic layers. This means that for the wavelike distribution of (2.19) there is a positive integer L such that

$$L\mathbf{q}_0=\mathbf{G}_b , \tag{3.1}$$

where $\mathbf{G}_b$ is one of the basis vectors of the reciprocal lattice of the pure crystal. Because of the wavelike nature of the impurity distribution, electronic wave vectors are defined to modulo $\mathbf{q}_0$ and the original Brillouin zone is partitioned into $2L-1$ regions. The folding of the original energy bands into the region centered at $\mathbf{k}=0$, which is the superlattice BZ, yields the subbands of the superlattice in the lowest approximation. Thus, there are L subbands associated with each original band. Figure 3 shows the folding of an original BZ (along the superlattice axis) and the subband formation for $L=2$. For $L=2$, the original BZ is partitioned into three regions: the center region, which becomes the superlattice BZ, and the two

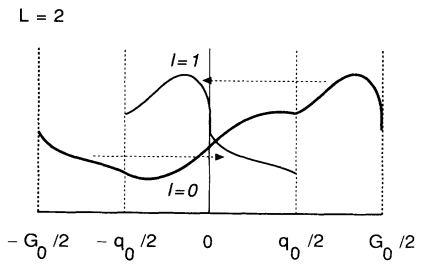

FIG. 3. Folding of the original BZ for $L=2$. The region bounded by $-q_0/2$ and $q_0/2$ forms the superlattice BZ. $l=0,1$ designate the two subbands.

side regions, which together form another zone. The thick line illustrates an arbitrary band energy. Since the original band energies are periodic in the reciprocal lattice space, $E_n^0(\mathbf{k}+\mathbf{G})=E_n^0(\mathbf{k})$, the ends of this curve at $G_0/2$ and $-G_0/2$ must have the same value. The pieces of the original curve that are in the central region to begin with form the first subband, which may be labeled $l=0$. The pieces that fall into the side regions form the second subband when they are transported into the central region. This second subband may be labeled $l=1$. Note that if L is even, there is always one zone that consists of two pieces that are graphically separated but border the surfaces the old BZ. I must emphasize here the qualification "graphically." Although in Fig. 3 the two regions on the left and right are separated graphically, they neighbor each other geometrically, because the boundary points $-G_0/2$ and $G_0/2$ are identical in the original BZ. If L is odd, the higher zones consist of pieces that neighbor each other on the graph. Figure 4 shows the partitioning of the original BZ for $L=3$. There are five partition regions and three zones. The three zones may be associated with $\mathbf{k}=\kappa+\mathbf{q}_0$, $\mathbf{k}=\kappa$, and $\mathbf{k}=\kappa-\mathbf{q}_0$, where $\kappa\in$ superlattice BZ. When the original band energy is folded into the superlattice BZ, one may label the resulting subbands $l=0$, $l=-1$, and $l=1$. Thus, for an arbitrary odd L, $\mathbf{k}$ is reduced to the superlattice BZ by setting

$$\mathbf{k}=\kappa+l\mathbf{q}_0 , \tag{3.2a}$$

where l is an integer confined to the interval

$$-\frac{(L-1)}{2}\le l\le\frac{(L-1)}{2} . \tag{3.2b}$$

After the reduction of (3.2a), the quantum numbers become

$$b=(nl\kappa s) . \tag{3.2c}$$

Figure 5 shows the partitioning of the original BZ for $L=4$. The zones are indicated on the figure. The reduction of $\mathbf{k}$ in the first three zones may be carried out exactly as above for the case of $L=3$. In the fourth zone, one may set $\mathbf{k}=\kappa\pm2\mathbf{q}_0$. Note that either $\kappa+2\mathbf{q}_0$ or $\kappa-2\mathbf{q}_0$ belongs to the original BZ, but not both at the same time. We may indicate these two possibilities by the following step function:

$$\Theta_{\mathrm{BZ}}(\mathbf{p})=\begin{cases}1 & \text{if } \mathbf{p}\epsilon \text{ original BZ}\\ 0 & \text{otherwise .}\end{cases} \tag{3.3}$$

One may now label as $l=2$ the subband associated with the reduction $\mathbf{k}=\kappa\pm2\mathbf{q}_0$. Thus, for an arbitrary even L,

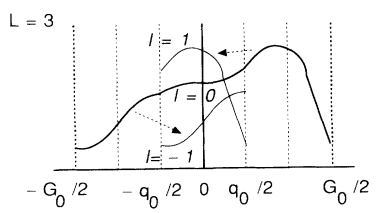

FIG. 4. The BZ folding for $L=3$.

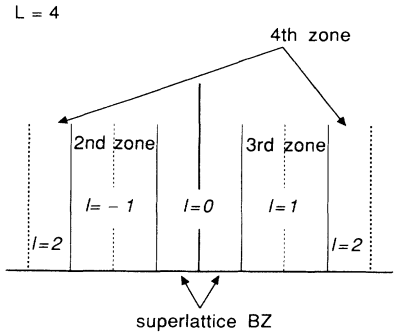

FIG. 5. The higher-superlattice BZ's for $L=4$.

the reduction of $\mathbf{k}$ may be carried out as follows:

$$\begin{aligned}\mathbf{k}&=\kappa+l\mathbf{q}_0 \ \text{ for } -\frac{(L-2)}{2}\le l\le\frac{(L-2)}{2} ,\\ \mathbf{k}&=\left[\kappa-\frac{L}{2}\mathbf{q}_0\right]\Theta_{\mathrm{BZ}}\left[\kappa-\frac{L}{2}\mathbf{q}_0\right]\\ &\quad+\left[\kappa+\frac{L}{2}\mathbf{q}_0\right]\Theta_{\mathrm{BZ}}\left[\kappa+\frac{L}{2}\mathbf{q}_0\right] \ \text{ for } l=\frac{L}{2} .\end{aligned} \tag{3.4a}$$

The corresponding subbands may be labeled by the integers

$$l=-\frac{(L-2)}{2},\ -\frac{(L-2)}{2}+1,\ \ldots,\ \frac{(L-2)}{2};\ \ \frac{L}{2} . \tag{3.4b}$$

The modified quantum numbers are again given by (3.2c), provided l is given by (3.4b). In the rest of the discussion, I will assume that L is odd. Some of the following formulas may require modification if L is even. This is discussed in Appendix A.

In terms of the modified quantum numbers, $W_{bb'}$ of Eq. (2.22) becomes

$$\begin{aligned}W_{nl\kappa;n'l'\kappa'}=\delta_{\kappa,\kappa'}W_0\sum_{\mathbf{G}}\{&\delta_{l,l'+1}\phi_n^*(\kappa+l\mathbf{q}_0-\mathbf{G})\\ &\times\phi_{n'}(\kappa+(l-1)\mathbf{q}_0-\mathbf{G})\\ &+\delta_{l+1,l'}\phi_n^*(\kappa+l\mathbf{q}_0-\mathbf{G})\\ &\times\phi_{n'}(\kappa+(l+1)\mathbf{q}_0-\mathbf{G})\} .\end{aligned} \tag{3.5}$$

Let us consider just the first two terms in (2.1). Let

$$H_{\mathrm{SL}}\equiv H_e+H_i . \tag{3.6}$$

From (3.5), one finds

$$\begin{aligned}H_{\mathrm{SL}}=&\sum_{n,l,\kappa}E_{nl\kappa}^0c_{nl\kappa}^\dagger c_{nl\kappa}\\ &+W_0\sum_{n,n',l,\kappa}[\Phi_{nn'}(l;\kappa)c_{n,l+1,\kappa}^\dagger c_{n'l\kappa}+\mathrm{H.c.}] ,\end{aligned} \tag{3.7a}$$

where

$$E_{nl\kappa}^0=E_n^0(\kappa+l\mathbf{q}_0) , \tag{3.7b}$$

$$\Phi_{nn'}(l;\kappa)=\sum_{\mathbf{G}}\phi_n^*(\kappa+(l+1)\mathbf{q}_0-\mathbf{G})\phi_{n'}(\kappa+l\mathbf{q}_0-\mathbf{G}) . \tag{3.7c}$$

$H_{\rm SL}$ may be diagonalized by means of a canonical transformation. Let $\hat{U}$ and $\hat{S}$ be operators such that

$$\hat{U}=e^{i\hat{S}},\quad \hat{S}=\sum_{b,b'}S_{bb'}C_b^\dagger C_{b'} , \tag{3.8}$$

where $C_b, C_b^\dagger$ are the electron operators in the representation which diagonalizes $H_{\rm SL}$. Let U and S stand for the matrices corresponding to $\hat{U}$ and $\hat{S}$. U is unitary; S is Hermitian. I will postulate that the old and the modified electron operators are related by the transformation

$$c_b=e^{-i\hat{S}}C_b e^{i\hat{S}} . \tag{3.9}$$

Expanding this expression in terms of the nested commutators of $\hat{S}$ with C_b, one readily finds that

$$c_b=\sum_{b'}U_{bb'}C_{b'},\quad U_{bb'}=(e^{iS})_{bb'} . \tag{3.10}$$

(3.10) is a Bogolubov transformation. $H_{\rm SL}$ in the modified representation is given by

$$H_{\rm SL}=e^{-i\hat{S}}H'_{\rm SL}e^{i\hat{S}}=H'_{\rm SL}+i[H'_{\rm SL},\hat{S}]+\frac{(i)^2}{2}([H'_{\rm SL},\hat{S}],\hat{S})+\cdots , \tag{3.11}$$

where $H'_{\rm SL}=H'_e+H'_i$ is the Hamiltonian of (3.7a) in which the operators c_b and $c_b^\dagger$ are replaced by C_b and $C_b^\dagger$.

The transformation (3.11) can be carried out approximately. If we choose $\hat{S}$ such that its commutator with H'_e cancels H'_i,

$$H'_i=-i[H'_e,\hat{S}] , \tag{3.12}$$

then the electronic eigenenergies are produced to $O(W_0^3)$ and the eigenstates to $O(W_0^2)$. If

$$S_{nl\kappa;n'l'\kappa'}=\frac{iW_0\delta_{\kappa\kappa'}}{E^0_{nl\kappa}-E_{n'l'\kappa}}[\Phi_{nn'}(l-1;\kappa)\delta_{l',l-1}+\Phi^*_{n'n}(l;\kappa)\delta_{l',l+1}] , \tag{3.13}$$

then (3.12) is satisfied. To $O(W_0^3)$, $H_{\rm SL}$ is given by

$$H_{\rm SL}=H'_e+\frac{i}{2}[H'_i,\hat{S}] . \tag{3.14}$$

Evaluating the commutator, one has

$$H_{\rm SL}=\sum_{n,l,\kappa}E_{nl\kappa}C^\dagger_{nl\kappa}C_{nl\kappa}+\sum_{n,l,n',l',\kappa}R_{nl;n'l'}(\kappa)C^\dagger_{nl\kappa}C_{n'l'\kappa} , \tag{3.15}$$

where

$$E_{nl\kappa}=E^0_{nl\kappa}-W_0^2\sum_{n''}\left[\frac{|\Phi_{nn''}(l-1;\kappa)|^2}{E^0_{n'',l-1}-E^0_{nl}}+\frac{|\Phi_{n''n}(l;\kappa)|^2}{E^0_{n'',l+1}-E^0_{nl}}\right] , \tag{3.16}$$

$$\begin{aligned}R_{nl;n'l'}(\kappa)=-\tfrac{1}{2}W_0^2\sum_{n''}\Bigg\{&[\delta_{l-2,l'}\Phi_{nn''}(l-1;\kappa)\Phi_{n''n'}(l-2;\kappa)+\delta_{ll'}(1-\delta_{nn'})\Phi_{nn''}(l-1;\kappa)\Phi^*_{n'n''}(l-1;\kappa)]\\&\times\left[\frac{1}{E^0_{n'',l-1}-E^0_{nl}}+\frac{1}{E^0_{n'',l-1}-E^0_{n'l'}}\right]\\&+[\delta_{ll'}(1-\delta_{nn'})\Phi^*_{n''n}(l;\kappa)\Phi_{n''n'}(l;\kappa)+\delta_{l+2,l'}\Phi^*_{n''n}(l;\kappa)\Phi^*_{n'n''}(l+1;\kappa)]\\&\times\left[\frac{1}{E^0_{n'',l+1}-E^0_{nl}}+\frac{1}{E^0_{n'',l+1}-E^0_{n'l'}}\right]\Bigg\} .\end{aligned} \tag{3.17}$$

$E_{nl\kappa}$ is the electronic eigenenergy to $O(W_0^3)$. $R_{nl;n'l'}$ represents the electron-impurity coupling left over because of the approximate nature of the transformation (3.13). I should point out that (3.13) is valid only if the zeroth-order subband energies $E^0_{nl\kappa}$ are not degenerate. In case of degeneracy, the elements of the transformation matrix must be obtained from the degenerate perturbation theory. One way to handle degeneracy is discussed in Appendix B.

Let us consider (3.16). Let l be positive. Assume that the original band is parabolic. To avoid problems associated with degeneracy, let us also assume that κ is finite. To zeroth order, the subband energies are given by

$$E^0_{nl\kappa}=E^0_n(0)+\frac{\hbar^2(\kappa+l\mathbf{q}_0)^2}{2m_n^*} . \tag{3.18}$$

Since κ is confined to the superlattice BZ, one has

$$\begin{aligned}&\kappa\cdot\mathbf{q}_0\le\tfrac{1}{2}\mathbf{q}_0^2 ,\\&2l\kappa\cdot\mathbf{q}_0\le l\mathbf{q}_0^2<l^2\mathbf{q}_0^2\end{aligned} \tag{3.19}$$

for $l>1$. Therefore, the subband energy is determined in the zeroth order largely by the term proportional to l^2:

$$E^0_{nl}\sim E^0_n(0)+\frac{\hbar^2l^2q_0^2}{2m_n^*} . \tag{3.20}$$

As one goes higher in the subband ladder, the separation of the steps increases:

$$E^0_{n,l+1,\kappa}-E^0_{nl\kappa}=\frac{\hbar^2}{2m_n^*}[2\kappa\cdot\mathbf{q}_0+(2l+1)q_0^2]\ . \tag{3.21}$$

The subband separation is proportional to l. Note that on the basis of (2.23b), one might expect that the electron should act like a harmonic oscillator, at least in the troughs of the potential field. (3.21) shows that the electron actually acts like an anharmonic oscillator.

If we take just two parabolic bands, one conduction and one valence, and consider the radiative interband transitions corresponding to the same l, we find that absorption (or luminescence) peaks are at

$$\hbar\omega\sim E_G+\frac{\hbar^2l^2q_0^2}{2}\left[\frac{1}{m_c^*}+\frac{1}{m_v^*}\right]\ . \tag{3.22}$$

Note that in the parabolic-band approximation, the subbands corresponding to $l=|l|$ and $l=-|l|$ may be close to each other for small κ. Their separation is given by

$$\delta E=\frac{2|l|\hbar^2\kappa\cdot\mathbf{q}_0}{m_n^*}\ . \tag{3.23}$$

Thus, the peaks of (3.22) are broadened if κ is small; they are split if κ is sufficiently large.

(3.20) indicates that the zeroth-order subband separation may be substantial if the impurity modulation wavelength $\Lambda_0=2\pi/q_0$ is short. If $\Lambda_0=50$ Å and $m^*=0.1$ m, then $\hbar^2q_0^2/(2m^*)\approx0.5$ eV. This suggests that one may rapidly run out of room in the original BZ for a valid parabolic-band approximation, since typical bandwidths are on the order of a few eV. A reasonable rule is that if $\Lambda_0<100$ Å, one should use the actual dispersion relation of the original band.

Next, let us consider the correction term arising from the impurity potential in (3.16). Let us denote it by δW_{nl}. δW_{nl} is proportional to W_0^2. Since W_0 is proportional to the impurity density N_0, this may suggest that δW_{nl} is proportional to N_0^2. However, W_0 also depends on the inverse screening length q_s, which is determined by the density of the free carriers. If the free-carrier distributions tend to follow the impurity distribution, then q_s will also depend on N_0. If one uses the Thomas-Fermi model of screening and assumes that there are just two symmetric bands, then one may approximate q_s by

$$q_s^2=\frac{4e^2m^*(3N_0)^{1/3}}{\hbar^2\pi^{1/3}}\ . \tag{3.24}$$

Therefore, two distinct N_0 dependences are possible for δW_{nl}:

$$\delta W_{nl}\propto\begin{cases}N_0^2 & \text{if } q_0>q_s\\ N_0^{4/3} & \text{if } q_0<q_s\ .\end{cases} \tag{3.25}$$

The regimes $q_0>q_s$ and $q_0<q_s$ may be called the weak and strong screening regimes, respectively. For $q_0>q_s$, the influence of an impurity is felt by carriers outside the superlattice cell in which the impurity is located. For $q_0<q_s$, the influence of an impurity is confined to distances less than the width of a superlattice cell. If one assumes that $N_0\sim10^{18}$ cm^{-3} and $m^*\sim0.1$, then $q_s\sim10^7$ cm^{-1}. For the simple Thomas-Fermi model, the period $\Lambda_0=100$ Å corresponds to the transition regime $q_0\sim q_s$.

Before we leave the subject of screening, two remarks are in order. First, if $N_A\neq N_D$, and/or the conduction and the valence bands are not symmetric, then the estimate (3.24) cannot be used for q_s. Even for $N_A=N_D=N_0$, (3.24) is a rough estimate for q_s. Because of the reduction in effective bandwidths when bands are split into subbands, one may expect the electron-hole liquid to be sluggish and ineffective in screening individual impurity charges. q_s needs to be calculated self-consistently, taking into account the reduction of the BZ. This may yield a much lower calculated value for q_s. Second, q_s depends on the free-carrier density, which may decouple from the impurity density under, for example, photoexcitation or carrier injection. In such cases q_s needs to be calculated self-consistently as well.

In the parabolic band approximation, the magnitude of δW_{nl} can be quite small, since W_0 is a small energy on the order of 10^{-3} eV. If $N_0\approx10^{18}$ cm^{-3}, $\epsilon_0\approx10$, and $(q_s^2+q_0^2)\approx10^{14}$ cm^{-2}, then $W_0\approx1.7\times10^{-3}$ eV. To estimate the terms multiplying W_0^2 in (3.16), we may expand the overlap function $\Phi_{nn'}(\mathbf{k};\mathbf{q})$ in powers of $\mathbf{q}$. This expansion is given in Appendix C. Using (C5), (C7), and (3.18), one finds for the two-band model

$$\delta W_{cl\kappa}\approx\frac{4m^*W_0^2}{\hbar^2q_0^2[2l+1+2\kappa\cdot\mathbf{q}_0q_0^{-2}][2l-1+2\kappa\cdot\mathbf{q}_0q_0^{-2}]}+\frac{2W_0^2\hbar^2q_0^2}{m^*E_G}\ . \tag{3.26}$$

If $\Lambda_0=200$ Å and $m^*=0.1$ m, then $2m^*W_0/(\hbar^2q_0^2)\approx0.05$. For band gaps on the order of 1 eV, (3.26) yields $|\delta W_{cl}|\leq10^{-4}$ eV. If $E^0_{n,l-1,\kappa}\sim E^0_{nl\kappa}$, or if the band gap goes to nearly zero (making the pure crystal a semimetal), δW_{nl} may become larger. However, in this case, the transformation (C6) is not well defined because of near degeneracy and one should use the method discussed in Appendix B.

Two further points should be noted. First, nonparabolic and nearly degenerate band structures may be manufactured by making the pure crystal itself a layered superlattice. Second, the discussion above makes it clear that the main function of shallow impurities is to break the symmetry of the pure crystal. The impurity potential is typically too weak to induce much of a spectral structure.

IV. COUPLING TO LIGHT

This section discusses the effect of the wavelike impurity distribution on the electron-photon coupling. In the following discussion, I assume that $\mathbf{q}_0$ is much larger than photon momenta and neglect radiative recoil. To $O(W_0^2)$, the linear electron-photon coupling Hamiltonian becomes

$$H_{e\gamma}=H'_{e\gamma}+i[H'_{e\gamma},\hat{S}]$$

$$=\sum_{n,n',l,\kappa,\mu}\{[g^{\mu}_{nn'}(l;\kappa)C^{\dagger}_{nl\kappa}C_{n'l\kappa}a_{\mu}+\text{H.c.}]$$

$$+[G^{\mu}_{nn'}(l;\kappa)C^{\dagger}_{n,l+1,\kappa}C_{n'l\kappa}$$

$$\times(a_{\mu}+a^{\dagger}_{\mu})+\text{H.c.}]\}\ , \tag{4.1a}$$

where

$$g^{\mu}_{nn'}(l;\kappa)=\frac{eA_{\mu}}{mc}\boldsymbol{\varepsilon}_{\mu}\cdot\mathbf{p}_{nn'}(\kappa+l\mathbf{q}_0)\ , \tag{4.1b}$$

and

$$G^{\mu}_{nn'}(l;\kappa)=W_0\sum_{n''}\left[\frac{g^{\mu*}_{n'n''}(l;\kappa)\Phi_{nn''}(l;\kappa)}{E^0_{n,l+1,\kappa}-E^0_{n''l\kappa}}+\frac{g^{\mu*}_{n''n}(l+1;\kappa)\Phi_{n''n'}(l;\kappa)}{E^0_{n'l\kappa}-E^0_{n'',l+1,\kappa}}\right]. \tag{4.1c}$$

All radiative transitions in (4.1a) take place at the same wave vector, since radiative recoil is neglected. The first group of terms, which are proportional to the coupling constant g, is stronger than the second group proportional to G. The latter is reduced relative to the first by the ratio of W_0 to a band gap or to a subband separation.

Consider the first group. Only subbands having the same l label are coupled, although their band indices may differ. If $n\neq n'$, then $\mathbf{p}_{nn'}$ is given by the interband momentum matrix element, whose wave-vector dependence may be neglected in III-V semiconductors. This implies that $g^{\mu}_{nn'}$ is nearly independent of l and κ for $n\neq n'$. If there is any dependence on subbands, one would expect this dependence to be weak. The opposite is true if $n=n'$. If one uses the effective-mass approximation, g^{μ}_{nn} becomes[7]

$$g^{\mu}_{nn}(l;\kappa)=\frac{e\hbar A_{\mu}}{m^*_n C}\boldsymbol{\varepsilon}_{\mu}\cdot(\kappa+l\mathbf{q}_0)\ , \tag{4.2}$$

where m^*_n is the effective mass for the band n. The coupling coefficient becomes linearly dependent on l. Radiative transitions within the same band, as well as within the same subband, can take place only in association with another elementary excitation such as a phonon in order to conserve momentum. For these free-carrier absorptions,[7] the absorption coefficient varies as $l^2q_0^2$. Everything else being equal, the free-carrier absorption is stronger for higher subbands. Of course such a conclusion may be drawn only if the effective-mass approximation may be made for $\mathbf{p}_{nn}(\kappa+l\mathbf{q}_0)$. If the original band structure does not permit this, then the free-carrier absorption may have a more complicated relation to different subbands.

Consider the second group of terms. If one uses the expansion (C1), the leading term for $\Phi_{nn'}$ is $\delta_{nn'}$. Thus, to lowest order in q_0, $G^{\mu}_{nn'}$ is given by

$$G^{\mu}_{nn'}(l;\kappa)\simeq W_0\left[\frac{g^{\mu*}_{n'n}(l;\kappa)}{E^0_{n,l+1,\kappa}-E^0_{nl\kappa}}+\frac{g^{\mu*}_{n'n}(l+1;\kappa)}{E^0_{n'l\kappa}-E^0_{n',l+1,\kappa}}\right]. \tag{4.3}$$

Consider an interband transition and set $n=c$, $n'=v$, and $\kappa=0$. In the parabolic-band approximation, one has

$$G^{\mu}_{cv}\approx\frac{2W_0(m^*_c+m^*_v)}{\hbar^2q_0^2(2l+1)}g^{\mu}_{cv}(0)\ . \tag{4.4}$$

Thus, the matrix element is proportional to the square of the superlattice period. As one goes higher in the subband ladder, G^{μ}_{cv} decreases inversely with $|l|$. If one remains within the same band,

$$G^{\mu}_{nn}\approx\frac{2W_0eA_{\mu}}{c\hbar q_0^2(2l+1)}\boldsymbol{\varepsilon}_{\mu}\cdot\mathbf{q}_0\ , \tag{4.5}$$

where (4.2) is used. The matrix element is now linear in the modulation wavelength. Interestingly, it is also independent of the effective mass.

The interaction Hamiltonian (4.1a) couples a subband l either to itself or to $l'=l\pm1$. The $l\rightarrow l'=l\pm1$ transitions arise from the commutator $[H'_{e\gamma},\hat{S}]$. If higher-order commutators are kept in the canonical transformation (3.11), one may also obtain couplings among subbands whose indices differ by more than one. For example, the second-order commutator $[[H'_{e\gamma},\hat{S}],\hat{S}]$ generates couplings between l and $l'=l\pm2$. The strength of this coupling is reduced by the square of the ratio of W_0 to a subband separation or a band gap. We may summarize these results as follows. Let δE represent either a subband separation within the same band or a forbidden gap of the original pure crystal. There is a hierarchy of selection rules for the radiative transitions of impurity superlattices. The hierarchy depends on powers of $W_0/\delta E$. If $\Delta l=l-l'$, then

$$\begin{aligned}&\Delta l=0\ \text{ to }O(W_0/\delta E)\ ,\\ &\Delta l=\pm1\ \text{ to }O(W_0^2/\delta E^2)\ ,\\ &\Delta l=\pm2\ \text{ to }O(W_0^3/\delta E^3)\ ,\end{aligned} \tag{4.6}$$

etc. One should keep in mind that these selection rules are based on the assumption that there is no degeneracy in the folded BZ. If there are degeneracies, the strength of some radiative transitions may be affected.

Two further points should be noted. First, the existence of selection rules is not restricted to the wavelike impurity distribution. As we shall see in the next section, the piecewise-constant-impurity distribution also has a hierarchy of selection rules. Second, the existence of these selection rules contrasts with the quantum tunneling picture,[4] which does not yield any selection rule. Experimental observations reported to data are not sufficiently controlled and precise to decide between these two contrasting physical pictures.

Next consider $H_{e\gamma\gamma}$. Neglecting radiative recoil, using (2.10a), (2.10c), and (3.13), one readily verifies that

$$[H_{e\gamma\gamma},\hat{S}]=0 \ . \tag{4.7}$$

Therefore, to $O(W_0^3)$, $H_{e\gamma\gamma}$ is given by

$$H_{e\gamma\gamma}=\frac{e^2}{2mc^2}\sum_{n,l,\kappa} C^{\dagger}_{nl\kappa}C_{nl\kappa} \times \sum_{\mu,\mu'} \hat{\varepsilon}_{\mu}\cdot\hat{\varepsilon}_{\mu'} A_{\mu} A_{\mu'}[a_{\mu}(a_{\mu'}+a^{\dagger}_{\mu'}) +\text{H.c.}] \ . \tag{4.8}$$

Thus the light scattering from the electron-hole plasma of an impurity superlattice is influenced only by how various subbands are filled and where the Fermi surface is.

V. PIECEWISE-CONSTANT DISTRIBUTION

To simplify the algebra, let us assume that n and p layers have the same width $\Lambda/2$. Let us also assume that the crystal is compensated and the superlattice axis is along the z direction. From Fig. 2, one may write the piecewise-constant-impurity distribution as

$$\begin{aligned} p_D(z)&=N_0 \lim_{M\to\infty}\sum_{s=-M}^{+M}\left[\Theta\left[z-s\Lambda+\frac{\Lambda}{4}\right]-\Theta\left[z-s\Lambda-\frac{\Lambda}{4}\right]\right], \\ p_A(z)&=N_0 \lim_{M\to\infty}\sum_{s=-M}^{+M}\left[\Theta\left[z-s\Lambda+\frac{\Lambda}{2}\right]-\Theta\left[z-s\Lambda+\frac{\Lambda}{4}\right]+\Theta\left[z-s\Lambda-\frac{\Lambda}{4}\right]-\Theta\left[z-s\Lambda-\frac{\Lambda}{2}\right]\right], \end{aligned} \tag{5.1}$$

where the Θ's are step functions and s varies over integers. M is a large positive integer. If the macroscopic length of the structure is L_z, then there are $2M+1$ superlattice cells in L_z. Let s be an integer in the interval $-M\le s\le M$ and take the limit $M\to\infty$ after performing certain sums in the Fourier space (the reason for this extra care is to avoid convergence problems[8]). In order to determine $W_{bb'}$, one needs the Fourier transforms of $p_D(z)$ and $p_A(z)$. The Fourier transform of the step function is

$$\Theta(z)=-\frac{i}{2\pi}\int_{-\infty}^{+\infty}dq\frac{e^{iqz}}{(q-i\alpha)} \ , \tag{5.2}$$

where $\alpha\to 0^{\dagger}$. Using (5.2), one finds

$$\sum_{s=-M}^{M}\left[\Theta\left[z-s\Lambda+\frac{\Lambda}{4}\right]-\Theta\left[z-s\Lambda-\frac{\Lambda}{4}\right]\right]=\frac{1-e^{-iq\Lambda(2M+1)}}{(1-e^{-iq\Lambda})e^{-iq\Lambda M}} \ . \tag{5.3}$$

Let

$$M_0=2M+1 \tag{5.4}$$

represent the total number of the cells in the structure. The sum in (5.3) may be written as

$$\sum_{s=-M}^{+M}\left[\Theta\left[z-s\Lambda+\frac{\Lambda}{4}\right]-\Theta\left[z-s\Lambda-\frac{\Lambda}{4}\right]\right]=\frac{\sin\left[\frac{M_0q\Lambda}{2}\right]}{\sin\left[\frac{q\Lambda}{2}\right]} \ . \tag{5.5}$$

$p_D(z)$ becomes

$$p_D(z)=N_0\lim_{M_0\to\infty}\int_{-\infty}^{+\infty}\frac{dq}{2\pi}e^{iqz}\left[\frac{\sin\left[\frac{q\Lambda}{4}\right]}{(q-i\alpha)}\right]\times\frac{\sin\left[\frac{M_0q\Lambda}{2}\right]}{\sin\left[\frac{q\Lambda}{2}\right]} \ . \tag{5.6}$$

Since $p_D(z)$ can be written in terms of its Fourier transform as

$$p_D(z)=\frac{L_z}{2\pi}\int_{-\infty}^{+\infty}dq\, e^{iqz}P_D(q) \ , \tag{5.7}$$

one has

$$p_D(q)=N_0\lim_{M_0\to\infty}\frac{1}{L_z}\times\int_{-\infty}^{+\infty}dq\, e^{iqz}\left[\sin\left[\frac{q\Lambda}{4}\right]\Big/(q-i\alpha)\right]\times\frac{\sin\left[\frac{M_0q\Lambda}{2}\right]}{\sin\left[\frac{q\Lambda}{2}\right]} \ . \tag{5.8}$$

Consider the limit $M_0\to\infty$. In order to take this limit, one must also let $L_z\to\infty$, while keeping the ratio of M_0 to L_z constant, because this ratio represents the number of superlattice cells per unit length

$$\lim_{M_0\to\infty}\frac{M_0}{L_z}=\frac{1}{\Lambda} \ . \tag{5.9}$$

As $M_0\to\infty$, the last factor in (5.8) becomes a series of δ functions:

$$\lim_{M_0\to\infty}\sin\left[\frac{M_0 q\Lambda}{2}\right]\Big/\sin\left[\frac{q\Lambda}{2}\right]=\lim_{M_0\to\infty}M_0\sum_s\delta_{q,2\pi s/\Lambda}\ , \tag{5.10}$$

where s varies over all integers. (5.8) becomes

$$P_D(q)=\frac{N_0}{2\pi}\sum_s\left[\sin\left[\frac{\pi s}{2}\right]\Big/ s\right]\delta_{q,2\pi s/\Lambda}\ . \tag{5.11}$$

The same procedure yields

$$P_A(q)=-P_D(q)\ . \tag{5.12}$$

If the z axis coincides with one of the basis vectors of the reciprocal lattice of the pure crystal, then the integer s may be split into two parts:

$$s=l+\frac{\Lambda G_z}{2\pi}\ ,\qquad -\frac{1}{2}\left[\frac{\Lambda}{a}-1\right]\le l\le\frac{1}{2}\left[\frac{\Lambda}{a}-1\right]\ . \tag{5.13}$$

Here a is the lattice constant and G_z is a reciprocal lattice vector. Note that because of (5.4) and (5.5), Λ/a must be odd for the geometry of Fig. 2. The sum over s becomes

$$\sum_s=\sum_{G_z}\sum_l\ . \tag{5.14}$$

It is clear from (5.13) that l is the subband index and that there are Λ/a subbands for a given band.

Substituting the above results into (2.18), and using the fact that if k_z and k_z' are confined to the original BZ, then

$$\delta_{k_z-k_z'-G_z-G_z',2\pi l/\Lambda+G_z''}=\delta_{G_z-G_z',G_z''}\delta_{k_z-k_z',2\pi l/\Lambda}\ , \tag{5.15}$$

one obtains

$$W_{n\mathbf{k};n'\mathbf{k}'}=-\left[\frac{4e^2N_0}{\varepsilon_0}\right]\sum_{\mathbf{G},\mathbf{G}'}\phi_n^*(\mathbf{k}-\mathbf{G})\phi_{n'}(\mathbf{k}'-\mathbf{G}')\sum_{l''}\frac{\delta_{k_z-k_z',2\pi l''/\Lambda}}{\{(\mathbf{k}-\mathbf{k}'-\mathbf{G}+\mathbf{G}')_\perp^2+[(2\pi l'')/\Lambda+G_z-G_z']^2+q_s^2\}}\times\sin\left[\frac{\pi l''}{2}+\frac{\Lambda(G_z-G_z')}{4}\right]\Big/\left[l''+\frac{\Lambda(G_z-G_z')}{2\pi}\right]\ . \tag{5.16}$$

$\mathbf{k}$ is reduced to the superlattice BZ by setting

$$\mathbf{k}=\kappa+\hat{\mathbf{z}}\frac{2\pi l}{\Lambda}\ . \tag{5.17}$$

In the superlattice BZ, the Kronecker δ in (5.16) becomes

$$\delta_{k_z-k_z',2\pi l''/\Lambda}=\delta_{\kappa_z\kappa_z'}\delta_{l-l',l''}\ . \tag{5.18}$$

At this point one may make an approximation by noting that if $\mathbf{G}\neq\mathbf{G}'$, the matrix element in (5.16) is rapidly decreased because of the denominators. One may therefore set $\mathbf{G}=\mathbf{G}'$ and find

$$W_{nl\kappa;n'l'\kappa'}=-\delta_{\kappa_z\kappa_z'}\left[\frac{4e^2N_0}{\varepsilon_0}\right]\Phi_{nl\kappa;n'l'\kappa'}\frac{\sin\left[\frac{\pi}{2}(l-l')\right]}{(l-l')[(\kappa-\kappa')_\perp^2+(4\pi^2/\Lambda^2)(l-l')^2+q_s^2]}\ , \tag{5.19a}$$

where

$$\Phi_{nl\kappa;n'l'\kappa'}=\sum_G\phi_n^*\left[\kappa+\hat{\mathbf{z}}\frac{2\pi l}{\Lambda}-\mathbf{G}\right]\times\phi_{n'}\left[\kappa'+\hat{\mathbf{z}}\frac{2\pi l'}{\Lambda}-\mathbf{G}\right]\ . \tag{5.19b}$$

Note that from (2.16b) one has

$$\Phi_{nl\kappa;n'l\kappa}=\delta_{nn'}\ . \tag{5.20}$$

The diagonal elements in (5.19a) are therefore given by

$$W_{nl\kappa;nl\kappa}=-\frac{2\pi e^2N_0}{\varepsilon_0 q_s^2}\equiv-W_s\ . \tag{5.21}$$

Let

$$E^0_{nl\kappa}=E^0_n\left[\kappa+\hat{\mathbf{z}}\frac{2\pi l}{\Lambda}\right]-W_s \tag{5.22}$$

and

$$W'_{nl\kappa;n'l'\kappa'}=(1-\delta_{nn'}\delta_{ll'}\delta_{\kappa_\perp\kappa_\perp'})W_{nl\kappa;n'l'\kappa'}\ . \tag{5.23}$$

Because of (5.20),

$$W'_{nl\kappa;n'l\kappa}=0 \tag{5.24}$$

for all n and n'. Thus, $W_{bb'}$ is nonzero if $l\neq l'$, or $\kappa_\perp\neq\kappa_\perp'$, or both. The superlattice Hamiltonian becomes

$$H_{\rm SL}=H_e+H_i$$
$$=\sum_{n,l,\kappa} E^0_{nl\kappa}c^\dagger_{nl\kappa}c_{nl\kappa}$$
$$+\sum_{n,l,\kappa;n',l',\kappa'} W'_{nl\kappa;n'l'\kappa'}c^\dagger_{nl\kappa}c_{n'l'\kappa'} . \quad (5.25)$$

Note that because of the sine factor in (5.19a), the piecewise-constant-impurity distribution couples only those subbands whose indices either do not differ or differ by an odd integer:

$$\Delta l=l-l'=0 \text{ or odd integer} . \quad (5.26)$$

$W_{bb'}$ vanishes for other pairs. This leads to an interesting conclusion for parabolic bands. As I pointed out in the previous section, the lowest-order subband energies $E^0_{nl\kappa}$ for parabolic bands may become degenerate for the subbands $|l|$ and $-|l|$ as κ becomes small. From (5.22), one finds that $E^0_{nl\kappa}$ as a function of κ_z obtains its minimum at $\kappa_z=-\pi/\Lambda$ and its maximum at $\kappa_z=\pi/\Lambda$ for the subband $l=|l|$. On the other hand, for the subband $l=-|l|$ the minimum and the maximum are at $\kappa_z=\pi/\Lambda$ and $\kappa_z=-\pi/\Lambda$, respectively. The two subbands are degenerate at $\kappa_z=0$. Although there are second-order corrections to these bands, one would expect them to be small; hence, these pairs should remain nearly degenerate, since $W_{bb'}$ of (5.19) does not couple them. One then has two sets of states such that their energies cross each other as κ_z varies.

Next, let us consider the canonical transformation. In order to define a well-behaved operator $\hat{S}$ whose commutator with H_e cancels H_i, one needs to use a suitable approximation of (5.25), because if $n=n'$, $l=l'$, and $\kappa_\perp\neq\kappa'_\perp$, then W' is finite, and the energy denominator for the matrix S can approach zero as $\kappa'_\perp$ continuously approaches $\kappa_\perp$. One cannot then perform the canonical transformation perturbatively. To avoid this problem, let us restrict the second sum in (5.25) to the range of $\kappa'_\perp$ such that $|E^0_{nl\kappa_\perp}-E^0_{nl\kappa'_\perp}|>W_s$. On the other hand for the range of $\kappa'_\perp$ such that $|E^0_{nl\kappa_\perp}-E^0_{nl\kappa'_\perp}|<W_s$, let us take an average over $\kappa'_\perp$ of $W_{nl\kappa;nl\kappa'}$ in (5.19a) and add the correction to W_s (thus adding this part of the Hamiltonian to $E^0_{nl\kappa}$). W_s thus becomes

$$W'_s=W_s+\delta W_s , \quad (5.27a)$$

where

$$\delta W_s\approx W_s\ln\left[1+\frac{2m_n^* W_s}{\hbar^2 q_s^2}\right] . \quad (5.27b)$$

One can now proceed as before. For the piecewise-constant distribution, the matrix S is given by

$$S_{nl\kappa;n'l'\kappa'}=\frac{iW'_{nl\kappa;n'l'\kappa'}}{(E^0_{nl\kappa}-E^0_{n'l'\kappa'})} . \quad (5.28)$$

Carrying out the transformation, one finds

$$H_{\rm SL}=\sum_{n,l,\kappa} E_{nl\kappa}C^\dagger_{nl\kappa}C_{nl\kappa}$$
$$+\sum_{n,l,\kappa;n',l',\kappa'} R_{nl\kappa;n'l'\kappa'}C^\dagger_{nl\kappa}C_{n'l'\kappa'} , \quad (5.29)$$

where

$$E_{nl\kappa}=E^0_n\left[\kappa+\hat{z}\frac{2\pi l}{\Lambda}\right]-W'_s$$
$$-\sum_{n'l'\kappa'}\frac{|W'_{nl\kappa;n'l'\kappa'}|^2}{(E^0_{n'l'\kappa'}-E^0_{nl\kappa})} , \quad (5.30a)$$

$$R_{nl\kappa;n'l'\kappa'}=-\frac{1}{2}\sum_{n'',l'',\kappa''} W'_{nl\kappa;n''l''\kappa''}W'_{n''l''\kappa'';n'l'\kappa'}$$
$$\times\left[\frac{1}{E^0_{n'l''\kappa''}-E^0_{n'l'\kappa'}}+\frac{1}{E^0_{n''l''\kappa''}-E^0_{nl\kappa}}\right] . \quad (5.30b)$$

To first order in N_0, all the bands (and their subbands) are lowered by an amount $-W_s$ relative to the bands of the pure crystal by the potential field of the impurities. W_s depends on the square of a screening length r_s:

$$W_s=\frac{2\pi e^2N_0}{\varepsilon_0 q_s^2}\equiv\frac{2\pi e^2N_0r_s^2}{\varepsilon_0} . \quad (5.31)$$

Thus the effects of the impurity potential depend on the screening length r_s. r_s, itself, depends on N_0 and on subband widths, hence on Λ. However, the relationship between r_s and Λ is not simply linear. It is more complex, since the lowering of the bands and their subbands depends on the superlattice period Λ only indirectly, through the screening length. This conclusion significantly differs from Ref. 1. In the theory of Ruden and Döhler, the band gap of the crystal is reduced by

$$2V_0=\frac{\pi e^2N_0\Lambda^2}{4\varepsilon_0} . \quad (5.32)$$

Since the superlattice period Λ may be varied at will, the effective band gap of the crystal may be varied at will according to (5.32). In the present theory, it is not Λ that directly affects the lowering of the bands, but r_s. Furthermore, to first order in N_0, all of the bands and subbands are lowered by the same constant amount W_s. Light transitions probe only energy differences and therefore would not detect the constant shift $-W_s$ if the entire macroscopic sample were one long superlattice. However, if the impurity superlattice cells are sandwiched between two layers that are made of a different material, then $-W_s$ appears in the lineup of the bands between the superlattice crystal and the boundary layers. Light transitions may then detect such shifts. Clearly, the shifts observed in some luminescence experiments[9] and usually attributed to V_0 actually have a more subtle many-body origin. They may be associated with the filling of subbands and with the second-order corrections, in which the screening wave vector sets the scale, or with the re-

normalization of the original band gap of the pure crystal from the high density of free carriers. This band-gap renormalization is dynamic in origin and is not associated with the static impurity-charge distribution.

Next, let us consider the linear electron-photon coupling. Taking the denominator as indicated in (4.1a) and using (5.28), one finds

$$H_{e\gamma}=\sum_{nn'l\kappa\mu}\{[g^{\mu}_{nn'}(l;\kappa)C^{\dagger}_{nl\kappa}C_{n'l\kappa}a_{\mu}+\text{H.c.}] +[G^{\mu}_{nl\kappa;n'l'\kappa'}C^{\dagger}_{nl\kappa}C_{n'l'\kappa'}a_{\mu}+\text{H.c.})\}\ , \quad (5.33a)$$

where

$$G^{\mu}_{nl\kappa;n'l'\kappa'}=\sum_{n''}\left[\frac{W'_{nl\kappa;n''l'\kappa'}g^{\mu}_{n''n'}(l';\kappa')}{E^0_{nl\kappa}-E^0_{n''l'\kappa'}} +\frac{g^{\mu}_{nn''}(l;\kappa)W'_{n''l\kappa;n'l'\kappa'}}{E^0_{n'l'\kappa'}-E^0_{n''l\kappa}}\right]. \quad (5.33b)$$

The g terms are the same as for the wavelike distribution. They couple pairs of states which have the same wave vectors and the same subband indices. The G terms are different. They couple pairs of states that differ either in subband indices, or in wave vectors, or in both.

Using (5.24), one sees that an important contribution to the sum in (5.33b) comes from the case where $n''=n$, $l=l'$, but $\kappa_{\perp}\neq\kappa'_{\perp}$, which can be written as

$$\delta G=-\frac{W_s q_s^2 e A_{\mu}\boldsymbol{\varepsilon}_{\mu}\cdot\mathbf{p}_{nn'}[\boldsymbol{\kappa}'_{\perp}+\hat{\mathbf{z}}\kappa_z+\hat{\mathbf{z}}(2\pi l/\Lambda)]}{[q_s^2+(\kappa-\kappa')_{\perp}^2][E^0_{nl\kappa_z,\kappa_{\perp}}-E^0_{nl\kappa_z,\kappa'_{\perp}}]}\ . \quad (5.34)$$

This shows that a radiative interband transition does not need to be vertical in the momentum space if it is accompanied by an impurity scattering. Nearby momentum states may be strongly coupled, depending on the energy denominator. One should keep in mind, however, that the difference between $\kappa_{\perp}$ and $\kappa'_{\perp}$ is not allowed to be indefinitely small. As discussed before, (5.33) may be used only for $[E_{nl,\kappa_{\perp}}-E_{nl,\kappa'_{\perp}}]>W_s$.

For the wavelike distribution, the coefficient G coupled neighboring subband indices. For the piecewise-constant distribution, we have a different rule because of (5.26). G in (5.33a) couples pairs of states whose subband indices differ by 0 or by an odd integer. If one carries out the canonical transformation to higher orders, Δl may become an even integer, although such transitions would take place at a much reduced rate. Clearly, one again has a hierarchy of selection rules, in contrast to the quantum tunneling picture.

Finally, the commutator $[H'_{e\gamma\gamma},\hat{S}]$ vanishes in the recoilless radiative transition approximation as before. For the piecewise constant distribution, $H_{e\gamma\gamma}$ is the same as in (4.8) to $O(S^2)$.

At the present time, one may compare the preceding results with experiment only to orders of magnitude, since the commonly used semiconductors have a variety of degeneracies which must be evaluated for identification of spectral resonances and for quantitative comparison of their spacing. Furthermore, the spectral data reported to date usually involve some form of compositional plus impurity superlattices. In these structures, the impurity distribution has a complex form which cannot be approximated by a simple piecewise-constant distribution.

VI. CONCLUDING REMARKS

The basic conclusion of the preceding theory is that, if the atomic nature of impurity charges is taken into account rather than assuming that these charges form a continuous jellium, then subband structure arises from symmetry breaking. The interband absorption and emission spectrum should therefore display a hierarchy of selection rules. Furthermore, free-carrier absorptions or emissions should get stronger for higher subbands. Another conclusion is that the static potential field associated with impurity charges is not strong enough to induce the shifts in effective band gaps that are presently attributed to it. One should rather look for the source of these shifts in a dynamic renormalization process.

In this paper, I have not pursued such a renormalization effect, nor the effects of temperature and carrier scattering on symmetry breaking. In order to analyze such many-body effects, one needs to add the Coulomb-scattering Hamiltonian, as well as the electron-phonon coupling Hamiltonian, to (2.1). Hopefully, this will be done in the near future. Such an analysis is necessary in order to understand basic processes in impurity superlattices. Ruden and Döhler analyzed many-body effects on subbands by using the density-functional formalism.[2] They found a relatively small effect on subbands. However, the density-functional formalism does not take into account interband coupling. Furthermore, the effect of symmetry breaking on such an analysis is not clear at the present time, at least to this author. For these reasons, I consider conclusions based on the density-functional formalism to be suspect.

A basic result of the symmetry-breaking mechanism is that the number of subbands of an original band is given by L and Λ/a for the wavelike and the piecewise-constant probability distributions, respectively. These are usually large integers. However, only a relatively small number of subbands will be accessible to observation in a direct-band-gap semiconductor, depending upon where the Fermi surface is. In a semiconductor such as GaAs, the conduction-band energy has its lowest values near the center of the BZ. As one moves away from the central region, towards the boundaries of the BZ, the conduction-band energy increases. When these higher-energy regions are folded onto the superlattice BZ, they yield higher subbands. On the other hand, subbands which are associated with the folding of the central region of the original BZ are lower in energy. In GaAs, they are the ones that are accessible to observation, for example, in a luminescence experiment, because they usually lie below the Fermi surface.

The folding of the BZ for impurity superlattices leads to an interesting prediction for indirect-band-gap semiconductors. For semiconductors such as Si and Ge, the

conduction-band energy decreases as one moves toward the BZ boundaries in certain directions. If one were to make impurity superlattices of these materials, these regions of lower energy would be folded into the superlattice BZ, creating conduction and valence subbands separated by a direct band gap which would be approximately the same as the original indirect band gap. In other words, impurity layers would convert Si and Ge into a direct-band-gap material. Such a conversion, being a superlattice effect, would depend on the electronic mean free path in a given sample, as I pointed out in the introduction. In order to observe a possible indirect-band-gap–direct-band-gap conversion, this mean free path must be much longer than the superlattice period.

ACKNOWLEDGMENTS

I would like to take this opportunity to thank G. Dente, D. Depatie, C. Largent, A. Ongstad, N. Pchelkin, and M. Prairie for many useful conversations, and M. Elçi for technical assistance.

APPENDIX A: EVEN L

Consider $W_{bb'}$. For the subband indices

$$-\frac{(L-2)}{2} \le l,l' \le \frac{(L-2)}{2} , \tag{A1}$$

the matrix elements $W_{bb'}$ are the same as in (3.5). If one or both indices equal $L/2$, then

$$W_{n,L/2,\kappa;n'l'\kappa'}=\Theta_{\rm BZ}\left[\kappa-\frac{L}{2}\mathbf{q}_0\right]\delta_{\kappa\kappa'}\delta_{l',-(L-2)/2}W_0\sum_{\mathbf{G}}\phi_n^*\left[\kappa-\frac{L}{2}\mathbf{q}_0-\mathbf{G}\right]\phi_{n'}\left[\kappa-\frac{(L-2)}{2}\mathbf{q}_0-\mathbf{G}\right]$$
$$+\Theta_{\rm BZ}\left[\kappa+\frac{L}{2}\mathbf{q}_0\right]\delta_{\kappa\kappa'}\delta_{l',(L-2)/2}W_0\sum_{\mathbf{G}}\phi_n^*\left[\kappa+\frac{L}{2}\mathbf{q}_0-\mathbf{G}\right]\phi_{n'}(\kappa+\frac{(L-2)}{2}\mathbf{q}_0-\mathbf{G}) , \tag{A2}$$

$$W_{nl\kappa;n',L/2,\kappa'}=W^*_{n,L/2,\kappa';nl\kappa} , \tag{A3}$$

and

$$W_{n,L/2,\kappa;n',L/2,\kappa'}=0 . \tag{A4}$$

When l is confined to the interval in (A1), the portion of the superlattice Hamiltonian involving these subbands is still given by (3.7a). However, there will be additional terms in the Hamiltonian because of the subband $L/2$. Let $H_{\rm SL}^{\rm ev}$ be the superlattice Hamiltonian for even L. It can be written as

$$H_{\rm SL}^{\rm ev}=H_{\rm SL}+\Delta H_{\rm SL} . \tag{A5}$$

$H_{\rm SL}$ is given by (3.7a). $\Delta H_{\rm SL}$ is given by

$$\Delta H_{\rm SL}=E^0_{n,L/2,\kappa}c^\dagger_{n,L/2,\kappa}c_{n,L/2,\kappa}+\sum_{n,n',\kappa}(c^\dagger_{n,L/2,\kappa}c_{n',-(L-2)/2,\kappa}W_{n,L/2,\kappa;n',-(L-2)/2}$$
$$+c^\dagger_{n,L/2,\kappa}c_{n',(L-2)/2,\kappa}W_{n,L/2,\kappa;n',(L-2)/2}) , \tag{A6}$$

where

$$E^0_{n,L/2,\kappa}=\Theta_{\rm BZ}\left[\kappa+\frac{L}{2}\mathbf{q}_0\right]E^0_n\left[\kappa+\frac{L}{2}\mathbf{q}_0\right]+\Theta_{\rm BZ}\left[\kappa-\frac{L}{2}\mathbf{q}_0\right]E^0_n\left[\kappa-\frac{L}{2}\mathbf{q}_0\right] . \tag{A7}$$

The modification of other formulas is readily inferred from the above.

For the piecewise-constant distribution, the evenness or oddness of the number of subbands of a given band depends on M_0. The case of odd M_0 is treated in Sec. V. For even M_0, after taking the limit (5.9), the ratio Λ/a is an even integer. There are $\Lambda/a-1$ subbands which are labeled l in the range

$$-\frac{1}{2}\left[\frac{\Lambda}{a}-2\right]\le l\le\frac{1}{2}\left[\frac{\Lambda}{a}-2\right] . \tag{A8}$$

There are two pieces of the BZ left over, as in the case of the wavelike distribution, which together form a single zone. Corresponding to this zone, the integer s in (5.13) may be partitioned as

$$s=\pm\frac{\Lambda}{2a}+\frac{\Lambda G_z}{2\pi} . \tag{A9}$$

Thus the last subband may be labeled $l=\Lambda/2a$.

APPENDIX B: DEGENERACY

When a finite number of states is degenerate, they may be decoupled from the rest by means of a canonical transformation. Once isolated to the desired degree of accura-

cy, their finite-dimensional Hamiltonian may be diagonalized directly. To demonstrate the method, let us consider $H_{\rm SL}$:

$$H_{\rm SL}=\sum_b E_b^0 c_b^\dagger c_b+\sum_{b,b'} W_{bb'} c_b^\dagger c_{b'}' \ , \tag{B1}$$

where b is given by (3.3). Assume that a finite number of states is degenerate with the same energy. Let us denote this group by $\{B\}$ and the remaining states by $\{\beta\}$. Assume that $\{\beta\}$ are well separated from $\{B\}$ in energy. Dividing the set $\{b\}$ into two sets $\{\beta\}+\{B\}$, one may rewrite $H_{\rm SL}$ as

$$H_{\rm SL}=H_0^D+H_0^R+H_i^D+H_i^{DR}+H_i^R \ , \tag{B2a}$$

where

$$H_0^D=\sum_B E_B^0 c_B^\dagger c_B, \quad H_0^R=\sum_\beta E_\beta^0 c_\beta^\dagger c_\beta \ , \tag{B2b}$$

$$H_i^D=\sum_{B,B'} W_{BB'} c_B^\dagger c_{B'}, \quad H_i^R=\sum_{\beta,\beta'} W_{\beta\beta'} c_\beta^\dagger c_{\beta'} \ , \tag{B2c}$$

$$H_i^{DR}=\sum_{\beta,B}(W_{\beta B} c_\beta^\dagger c_B+W_{B\beta} c_B^\dagger c_\beta) \ . \tag{B2d}$$

One may perform a canonical transformation, as in (3.11), and remove H_i^{DR} to first order in $\hat{S}$ by picking an $\hat{S}$ such that

$$H_i^{DR'}=-i[H_0^{D'}+H_0^{R'},\hat{S}] \ . \tag{B3}$$

(B3) is satisfied if

$$\hat{S}=i\sum_{\beta,B}\left[\frac{W_{\beta B}}{E_\beta^0-E_B^0}C_\beta^\dagger C_B+\frac{W_{B\beta}}{E_B^0-E_\beta^0}C_B^\dagger C_\beta\right] . \tag{B4}$$

The modified superlattice Hamiltonian becomes

$$H_{\rm SL}=H_0^{D'}+H_0^{R'}+H_i^{D'}+i[H_i^{D'},\hat{S}]+\frac{i}{2}[H_i^{DR'},\hat{S}]+H_i^{R'}+i[H_i^{R'},\hat{S}]+\cdots \ . \tag{B5}$$

Consider

$$H_{\rm SL}^D\simeq H_0^{D'}+H_i^{D'}+\frac{i}{2}[H_i^{DR'},\hat{S}] \ . \tag{B6}$$

To $O(S^2)$, the degenerate states are decoupled from the rest. $H_{\rm SL}^D$ may be written as

$$H_{\rm SL}^D=\sum_{B,B'} M_{BB'} C_B^\dagger C_{B'} \ , \tag{B7a}$$

where

$$M_{BB'}=E_B^0\delta_{BB'}+W_{BB'}-\frac{1}{2}\sum_\beta W_{B\beta}W_{\beta B'}\left[\frac{1}{E_\beta^0-E_B^0}+\frac{1}{E_\beta^0-E_{B'}^0}\right] . \tag{B7b}$$

One can now diagonalize the finite-dimensional matrix M with a unitary transformation.

APPENDIX C: EXPANSION OF $\Phi_{nn'}$

The Taylor expansion with respect to $\mathbf{q}$ yields

$$\sum_G \phi_n^*(\mathbf{k}-\mathbf{G})\phi_{n'}(\mathbf{k}-\mathbf{G}-\mathbf{q})=\delta_{nn'}+iq_\lambda X_{nn'}^\lambda-\frac{i}{2}q_\lambda q_\mu\frac{\partial}{\partial k_\mu}X_{nn'}^\lambda-\frac{1}{2}q_\lambda q_\mu\sum_{n''}X_{nn''}^\mu X_{n''n'}^\lambda\cdots \ , \tag{C1}$$

where the repeated vector indices are summed over and $\mathbf{X}_{nn'}$ is the interband part of the position operator[6]

$$\mathbf{X}_{nn'}(\mathbf{k})=i\sum_G \phi_n^*(\mathbf{k}-\mathbf{G})\frac{\partial}{\partial\mathbf{k}}\phi_{n'}(\mathbf{k}-\mathbf{G}) \ . \tag{C2}$$

For the two-band model, $\mathbf{X}_{cv}$ is related to $\mathbf{p}_{cv}$ by

$$\mathbf{X}_{cv}=\frac{-i\hbar\mathbf{p}_{cv}}{m(E_c-E_v)} \ . \tag{C3}$$

For the two-band model, the f-sum rule[8] yields

$$\frac{|\mathbf{p}_{cv}|^2}{m^2E_G}\sim\frac{1}{m^*} \ , \tag{C4}$$

where E_G is the band gap and m^* is the effective mass. Thus,

$$|\mathbf{q}_0\cdot\mathbf{X}_{cv}|^2\sim\frac{\hbar^2q_0^2}{m^*E_G} \ . \tag{C5}$$

For $\Lambda_0\equiv(2\pi/q_0)\sim100$ Å, $E_G\sim1$ eV, and $m^*\sim0.1$ m, one finds $|\mathbf{q}_0\cdot\mathbf{X}_{cv}|^2\sim0.2$. If Λ_0 is around 40 Å, then this ratio rapidly rises to 1 and the expansion (C1) is not valid.

For (C1) and for $\mathbf{X}_{nn}=\mathbf{0}$ (the conditions under which this holds are discussed in Ref. 10); the elements of S are given by

$$S_{nl\kappa;n'l'\kappa'}=\frac{iW_0\delta_{\kappa\kappa'}}{E^0_{nl\kappa}-E^0_{n'l'\kappa}}\left[(\delta_{l,l'+1}+\delta_{l+1,l'})\left\{\delta_{nn'}-\frac{i}{2}\mathbf{q}_0\cdot\frac{\partial}{\partial\mathbf{k}}\mathbf{q}_0\cdot\mathbf{X}_{nn'}(l;\kappa)-\frac{1}{2}\sum_{n''}\mathbf{q}_0\cdot\mathbf{X}_{nn''}(l;\kappa)\mathbf{q}_0\cdot\mathbf{X}_{n''n'}(l;\kappa)\right\}\right.$$
$$\left.+(\delta_{l,l'+1}-\delta_{l+1,l'})[i\mathbf{q}_0\cdot\mathbf{X}_{nn'}(l;\kappa)]\right]. \tag{C6}$$

In this approximation, $E_{nl\kappa}$ becomes

$$E_{nl\kappa}=E^0_{nl\kappa}-W_0^2\left\{\frac{1}{E^0_{n,l-1,\kappa}-E^0_{nl\kappa}}\left[1-\frac{1}{2}\sum_{n'}[|\mathbf{q}_0\cdot\mathbf{X}_{nn'}(l-1;\kappa)|^2+|\mathbf{q}_0\cdot\mathbf{X}_{nn'}(l+1;\kappa)|^2]\right]\right.$$
$$+\frac{1}{E^0_{n,l+1,\kappa}-E^0_{nl\kappa}}\left[1-\frac{1}{2}\sum_{n'}[|\mathbf{q}_0\cdot\mathbf{X}_{nn'}(l;\kappa)|^2+|\mathbf{q}_0\cdot\mathbf{X}_{nn'}(l+1;\kappa)|^2]\right]$$
$$\left.+\sum_{n'}\left[\frac{\mathbf{q}_0\cdot\mathbf{X}_{nn'}(l;\kappa)\mathbf{q}_0\cdot\mathbf{X}_{n'n}(l-1;\kappa)}{E^0_{n'l-1,\kappa}-E^0_{nl\kappa}}+\frac{\mathbf{q}_0\cdot\mathbf{X}_{nn'}(l;\kappa)\mathbf{q}_0\cdot\mathbf{X}_{n'n}(l+1;\kappa)}{E^0_{n'l+1\kappa}-E^0_{nl\kappa}}\right]\right\}. \tag{C7}$$

[1]P. Ruden and G. H. Döhler, Phys. Rev. B **27**, 3538 (1983).
[2]P. Ruden and G. H. Döhler, Phys. Rev. B **27**, 3547 (1983).
[3]G. H. Döhler, IEEE J. Quantum Electron. **QE-22**, 1682 (1986).
[4]G. H. Döhler, H. Künzel, and K. Ploog, Phys. Rev. B **25**, 2616 (1982).
[5]R. Kubo, J. Phys. Soc. Jpn. **12**, 570 (1957).
[6]A. Elçi and E. D. Jones, Phys. Rev. B **34**, 8611 (1986).
[7]A. Elçi, M. O. Scully, A. L. Smirl, and J. C. Matter, Phys. Rev. B **16**, 191 (1977).
[8]A. Elçi, Phys. Rev. B **34**, 8616 (1986).
[9]E. F. Schubert, J. E. Cunningham, and W. T. Tsang, Phys. Rev. B **36**, 1348 (1987).
[10]A. Elçi (unpublished).